Case Studies in Thermal Engineering 4 (2014) 76–84

Contents lists available at ScienceDirect

Case Studies in Thermal Engineering

journal homepage: www.elsevier.com/locate/csite

Computational investigation of film cooling from cylindrical and row trenched cooling holes near the combustor endwall

Ehsan Kianpour, Nor Azwadi Che Sidik*

Department of Thermo Fluid, Faculty of Mechanical Engineering, University Technology Malysia, 81310 Skudai, Johor, Malaysia

ARTICLE INFO

Article history:
Received 29 April 2014
Received in revised form
15 June 2014
Accepted 10 July 2014
Available online 23 July 2014

Keywords:
Gas turbine
Film-cooling
Cylindrical hole
Trenched hole
Dilution hole

ABSTRACT

This study was performed to investigate the effects of cylindrical and row trenched cooling holes with alignment angles of 0° and 90° at blowing ratio of 3.18 on the film cooling performance adjacent to the endwall surface of a combustor simulator. In this research a three-dimensional representation of Pratt and Whitney gas turbine engine was simulated and analyzed with a commercial finite volume package FLUENT 6.2. The analysis has been carried out with Reynolds-Averaged Navier–Stokes turbulence model (RANS) on internal cooling passages. This combustor simulator was combined with the interaction of two rows of dilution jets, which were staggered in the streamwise direction and aligned in the spanwise direction. Film cooling was placed along the combustor liner walls. In comparison with the baseline case of cooling holes, the application of a row trenched hole near the endwall surface doubled the performance of film cooling effectiveness.

1. Introduction

Advanced gas turbine industries are striving for higher engine efficiencies, and Bryton cycle is the key to achieving this goal. According to this cycle, the turbine inlet temperature should increase to obtain more efficiency. However, the turbine inlet temperature enhancement formed an extremely harsh environment for critical downstream components such as combustor endwall surface and turbine vanes. Therefore, it is essential to plan a cooling scheme in this area. Film cooling is the usual way used. In this system, a thin thermal boundary layer is formed by cooling holes and attached to the protected surface. Cylindrical and trenched cooling holes are the two arrangements of the holes.

Hale et al. [1] measured the effectiveness of surface adiabatic film cooling adjacent to the cooling holes. They noted a variety of L/D ratios, injection angles as well as co-flow and counter-flow plenum feed configurations. The findings of their studies were compatible with the Burd and Simon [2] results which reported that short injection holes enhanced film cooling and created a larger cold area downstream of the cooling holes.

Stitzel and Thole [3] indicated that dilution jet injection is the dominant feature at the combustor exit, while without dilution, the exit profile was relatively uniform with high temperature and low total pressure flow in the mainstream. Furthermore, Scrittore [4] mentioned that increasing the dilution jet velocity adversely affects the surface cooling performance downstream of dilution jets.

Kianpour et al. [5,6] simulated and analyzed the effect of cooling holes geometry at the combustor endwall on the exit flow profiles. The results showed that the temperatures adjacent to the wall and between the jets were about seven percent

* Corresponding author.
E-mail addresses: ekianpour@gmail.com (E. Kianpour), azwadi@fkm.utm.my (N.A. Che Sidik).

http://dx.doi.org/10.1016/j.csite.2014.07.004

cooler with few cooling holes and wider cross-sectional area. In this condition, the coolant spread better near the endwall surface and a wide protected layer was created in order to save the surface against hot gases.

Aga and Abhari [7] and Chien et al. [8] investigated the effects of different inclinations and lateral angles of holes on film cooling effectiveness. They showed that the average adiabatic effectiveness is about twice for streamwise injection at large compound angles (60° and 90°) even for high blowing ratios.

Yiping et al. [9] and Maikell et al. [10] tested the effects of different trench depths and widths on the film cooling under overall cooling effectiveness of $\phi=0.6$. They figured out that $w=2.0D$ and $d=0.75D$ and $w=3.0D$ and $d=0.75D$ cases were more effective than the other cases. For the baseline case, the trench depth of $0.75D$ was optimum and approved by CFD studies.

Azzi and Jurban [11] used various techniques to detect the thermal characteristics of film cooling. In this study, they used standard k–ε turbulence model to solve the Reynolds-Averaged Navier–Stokes equation. In concurrence with Rozati and Danesh [12], the results showed that the film cooling effectiveness was modified at low blowing ratios.

Few researchers [13–16] studied the effects of trenched depth and width on film cooling performance at the vane endwall. Their results showed that the maximum cooling effectiveness is obtained at the trench depth of $0.80D$. However, Lawson and Thole [13] claimed that the trench depth of $0.8D$ has a negative effect on the cooling performance downstream of the cooling hole.

Liang et al. [17,18] conducted few tests to analyze the nonuniformities of temperature adjacent to the wall surfaces and film cooling effectiveness of converging slot hole (console) rows. They concentrated on the effectiveness of the distribution of film cooling using two different exits to inlet area ratios of converging slot hole. The results showed that the coolant injected from the converging slot was attached to the blade surface and enhanced heat transfer.

Somawardhana and Bogard [19] investigated the effects of shallow trenched holes ($h=0.5$ d) to modify film cooling effectiveness. The results were confirmed by Vakil and Thole [20] and Shupping [21] stated that higher film cooling effectiveness for the trenched holes resulted due to the net heat flux reduction that was more than the baseline case, while the heat transfer coefficients for both cases were almost constant.

It appears from the aforementioned investigations that numerous investigations have been conducted for the effects of cooling hole geometry, however, only one attempt was made to investigate the effect of trenching cooling holes near the combustor endwall surface [22,23]. This leads to several unanswered questions: How do trenched cooling holes modify the film cooling performance at the combustor endwall surface in comparison with cylindrical holes? How do cylindrical and trenched cooling holes perform at the same blowing ratios? Therefore, the purpose of the current study was to analyze the film cooling effectiveness variation with different arrangements of cooling holes. Also, in order to identify the validity of the findings, a comparison between the data attained from this investigation and the Vakil and Thole [20] project was carried out.

2. Methods and materials

In this research, a three-dimensional representation of a true Pratt and Whitney gas turbine engine was simulated and analyzed to obtain fundamental data. Fig. 1 shows the schematic view of the combustor. The combustor simulator length, width and inlet height were 156.9 cm, 111.8 cm and 99.1 cm, respectively. The contraction angle was 15.8° and it began at $X=79.8$ cm. While the inlet cross sectional area was 1.11 m^2, the exit cross sectional area was 0.62 m^2. The combustor contained four streamwise film cooling panels. The combustor simulator consisted of a streamwise series of four film-cooled panels, which were symmetrical on the top and bottom of the combustor simulator. These panels began approximately 2.7 vane chords (~1.57 m) upstream of the turbine test section. The first two panel lengths were 39 and 41 cm while the third and fourth panels were 37 cm and 43 cm, respectively. The panels were 1.27 cm in thickness. Theses panels were made from low thermal conductivity of combustor panels allowed for adiabatic surface temperature measurements.

The second and third cooling panels contained two different rows of dilution holes. These dilution rows were located at 0.67 m and 0.90 m downstream of the beginning of the combustor liner panels. The first and second rows of dilution holes diameter were 8.5 cm and 11.9 cm, respectively.

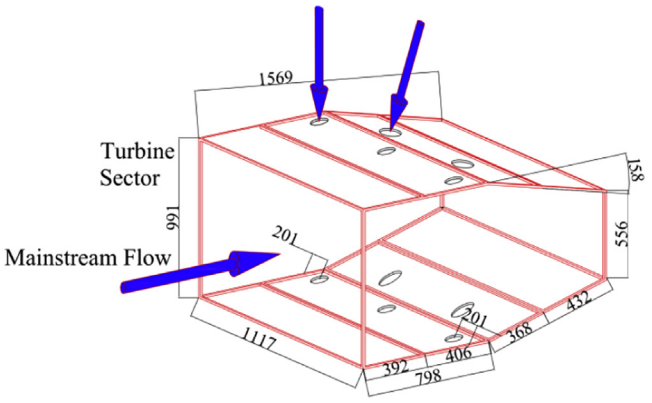

Fig. 1. The 3-D view of the combustor simulator.

In the present research, the combustor simulator included three configurations of cooling holes. For the verification of findings, the first arrangement (baseline or case 1) was planned similar to the Vakil and Thole [20] combustor simulator. For all the cases, the cooling holes were located in equilateral triangles. The diameter of the cooling holes was 0.76 cm and drilled at an angle of 30° from the horizontal surface. The length of each cooling hole in the baseline case was 2.5 cm. For the second and third cases shown in Fig. 2, the cooling holes were placed within a row trench with alignment angles of 0° (case 2) and 90° (case 3). According to the Yiping et al. [9], Lawson and Thole [13], and Sundaram and Thole [15] findings, the trench depth and width were considered to be equal to 0.75*D* and 1.0*D*, respectively. These researchers showed that the optimum film cooling effectiveness for the trenched cases was obtained among the narrower trench and the depth of ~0.75*D*. Furthermore, a variety of coolant blowing ratios from 1.25 to 3.18 was considered. A global coordinate system (*x*, *y*, and *z*) was also selected.

The distribution of film cooling effectiveness (η) inside the combustor simulator was measured along the specified measurement planes. The measurement planes are shown in Fig. 3a (baseline), b (case 2), and c (case 3). The flow field measurement planes of 0p, 1p, 2p, and 3p were located in pitchwise direction and the measurement plane of 0s was placed in the streamwise direction. Plane 0p was placed exactly downstream of the first panel of cooling holes and at $x=35.1$ cm. The momentum distribution of film cooling was determined along this panel. This measurement plane covered half of the combustor simulator in the spanwise direction. The height of the measurement plane covered 0 cm $< z <$ 10 cm.

Plane 1p was placed downstream of the first row of dilution jet at $x=74.85$ cm. This plane was expanded from $z=0$ cm to $z=10$ cm and covered the half width of the combustor simulator. This plane was used to detect the effects of film cooling on the dilution flow. This plane was also used to determine the effects of horseshoe, half-wake, and counter rotating vortexes. Plane 2p was located downstream of the trailing edge of the second row of dilution holes. This plane was embedded at $x=1.1$ cm and was expanded along the vertical axis from $z=0.09$ cm to 0.22 cm. The effects of the cooling holes located in this section on the thermal behavior were identified by this plane. Plane 3p was set at the end of the combustor simulator. The usage of this plane enabled the

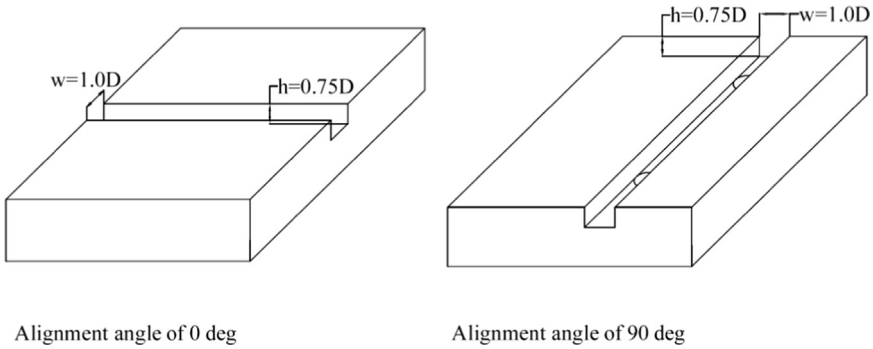

Fig. 2. The arrangement of trenched cooling holes with different alignment angles.

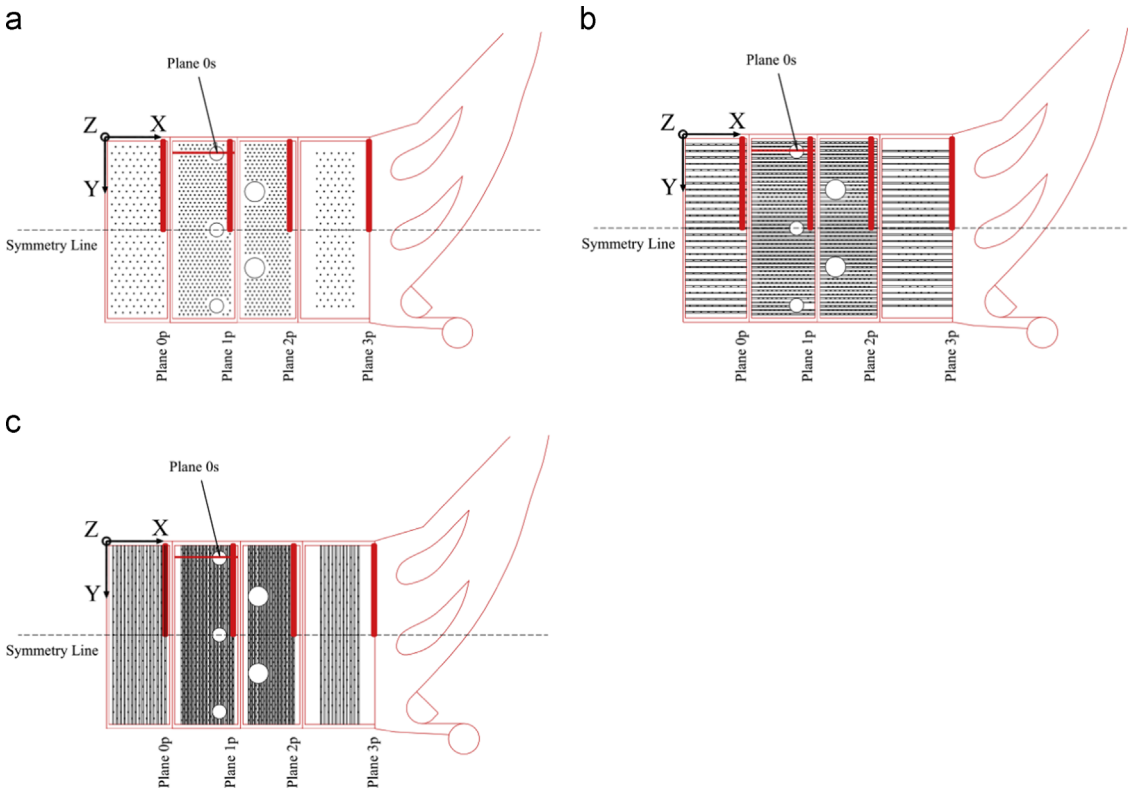

Fig. 3. Location of the measurement planes. (a) Baseline, (b) case 2, and (c) case 3.

researcher to detect the exit flow behavior and the varying temperature of the combustor. Plane 0s was located directly at the central point of the first row of dilution jet at $y=9.3$ cm and covered from $x=39.2$ cm to $x=78.45$ cm. This plane was used to analyze the interaction of flow along the first row of dilution jets.

About 8×10^6 tetrahedral meshes were needed to solve the combustor simulator problem and to attain more accurate data in inappropriate time. The usage of this number of meshes allowed adequate convergence for refined meshing. The precision of the number of meshes used in this research was in agreement with a study by Stitzel and Thole [3]. As demonstrated in Fig. 4, the meshes were denser around the cooling and dilution holes as well as on the wall surfaces.

According to the specified mass flux ratio at the inlet of volume control, inlet mass flow boundary condition was considered at the inlet. Wall boundary condition and slipless boundary condition were used to limit the interaction zone between the fluid and solid layers. In addition, to compare the outcomes of the present research with the previous findings as reported [3,20], the inlet flow boundary was set as uniform flow and pressure outlet at the exit.

In the current study, we considered a transient, incompressible turbulent flow ($\mathrm{Re}=2.2\times10^5$) by means of the RNG k–ε turbulent model of the Navier–Stokes equations expressed as follows:

Continuity equation:

$$\frac{\partial\rho}{\partial t}+\frac{\partial\rho}{\partial x}\frac{dx}{dt}+\frac{\partial\rho}{\partial y}\frac{dy}{dt}+\frac{\partial\rho}{\partial z}\frac{dz}{dt}=-\rho(\nabla.V) \tag{1}$$

Momentum equation:

$$\frac{\partial}{\partial t}(\rho u_i)+\frac{\partial}{\partial x_j}(\rho u_i u_j)=-\frac{\partial p}{\partial x_i}+\frac{\partial\tau_{ij}}{\partial x_i}+\rho g_i+\vec{F_i} \tag{2}$$

Energy equation:

$$\frac{\partial}{\partial t}(\rho E)+\frac{\partial}{\partial x_i}(u_i(\rho E+P))=\frac{\partial}{\partial x_i}\left(K_{eff}\frac{\partial T}{\partial x_i}-\sum_j h_j J_j+u_j(\tau_{ij})_{eff}\right)+S_h \tag{3}$$

and RNG k–ε equation:

$$\frac{\partial}{\partial t}(\rho k)+\frac{\partial}{\partial x_i}(\rho k u_i)=\frac{\partial}{\partial x_j}\left[\left(\mu+\frac{\mu_t}{\sigma_k}\right)\frac{\partial k}{\partial x_j}\right]+P_k-\rho\varepsilon \tag{4}$$

$$\frac{\partial}{\partial t}(\rho\varepsilon)+\frac{\partial}{\partial x_i}=(\rho\varepsilon u_i)=\frac{\partial}{\partial x_j}\left[\left(\mu+\frac{\mu_t}{\sigma_\varepsilon}\right)\frac{\partial\varepsilon}{\partial x_j}\right]+C_{1\varepsilon}\frac{\varepsilon}{k}P_k-C^*_{2\varepsilon}\rho\frac{\varepsilon^2}{k} \tag{5}$$

To understand the thermal field results, the film cooling effectiveness is defined as below

$$\eta=\frac{T-T_\infty}{T_C-T_\infty} \tag{6}$$

Here, T is the local temperature, T_∞ is the main stream temperature and T_C is the temperature of the coolant.

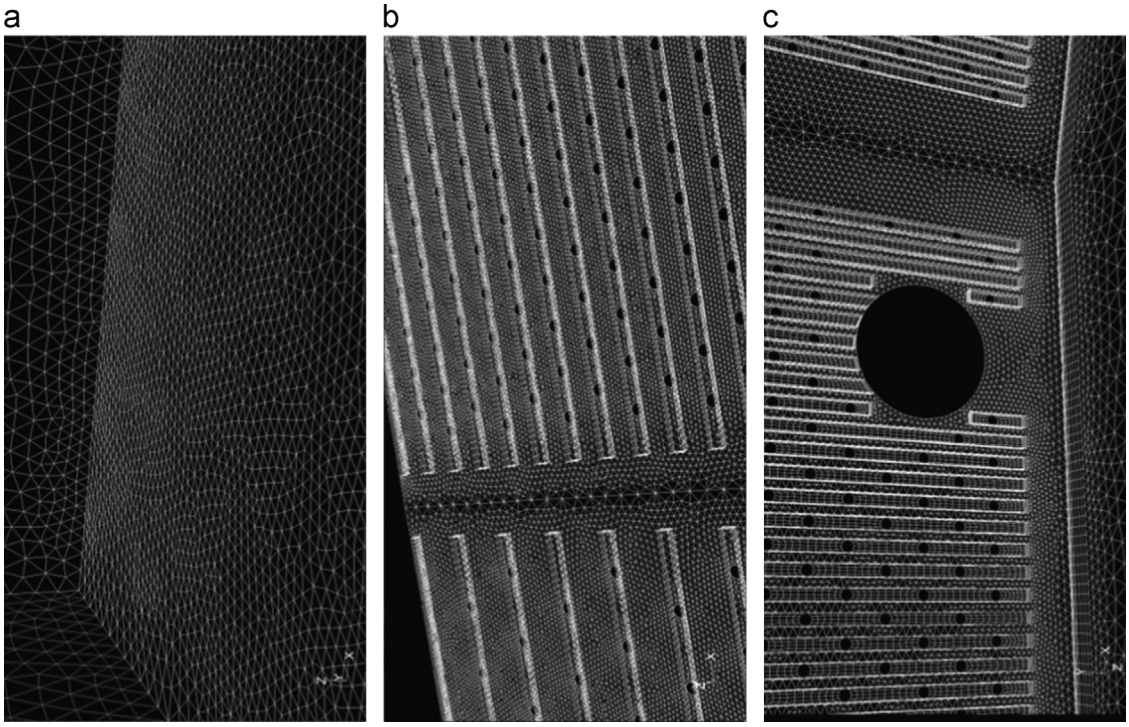

Fig. 4. Three-dimensional meshes of combustor simulator. (a) Baseline, (b) case 2, and (c) case 3.

3. Findings and discussion

A comparison was done between the current study results and the numerical findings gathered by Stitzel and Thole [3] and experimental results collected by Vakil and Thole [20]. Fig. 5 presents the comparison of film cooling effectiveness for plane 1p and 2p at $y/W=0.4$. Deviations between the current computation and benchmarks were calculated as follows:

$$\%Diff = \frac{\sum_{i=1}^{n} \frac{x_i - x_{i,benchmark}}{x_{i,benchmark}}}{n} \times 100 \quad (7)$$

According to this equation, the deviation estimation was 9.76% and 8.34% compared to Refs. [20] and [3] for plane 1p and equal to 13.36% and 11.96% in comparison with Refs. [20] and [3] for plane 2p.

The film cooling distribution for plane 0p is shown in Fig. 6a (baseline), b (case 2) and c (case 3). A noticeable difference between these figures is the film cooling layer thickness. For the baseline case, the thickness of this layer reached $Z=3.8$ cm. However, for the trenched case with alignment angles of 0° and 90°, it reached $Z=2.4$ cm and $Z=6$ cm, respectively. However, for this measurement plane, the thicker film cooling layer for the trenched hole does not automatically suggested that it is desirable. As seen in the trenched case with alignment angle of 90° and at a position of 31 cm $< Y <$ 36 cm, the temperature level is higher near the endwall surface. Furthermore, upon closer investigation, it looks as though the temperatures between the jets and near the wall are cooler for the trenched hole with alignment angle of 0°. This variation of temperature, however, does not have an effect on the density and viscosity of the flow fields.

The distribution of film cooling effectiveness for plane 1p is shown in Fig. 7a (baseline), b (case 2) and c (case 3). Note that the film cooling was significantly increased between these two cases. Fig. 7a shows the high temperature near the endwall surface compared to the trenched cases. However, no dominant cooling modifications are seen along the linear wall. Just at the right side of Fig. 7a and b (50 cm $< Y <$ 54 cm), the thermal field contours show that film cooling is being entrained by the upward motion of dilution jet. Also, at the position of 18 cm $< Y <$ 40 cm and 8 cm $< Z <$ 10 cm is slightly hotter ($0 < \eta < 0.05$) for the trenched case with alignment angle of 90° as opposed to the baseline. However, adjacent to the endwall surface, this kind of trenched hole performs better compared to other cases. The v and w velocity vectors of plane

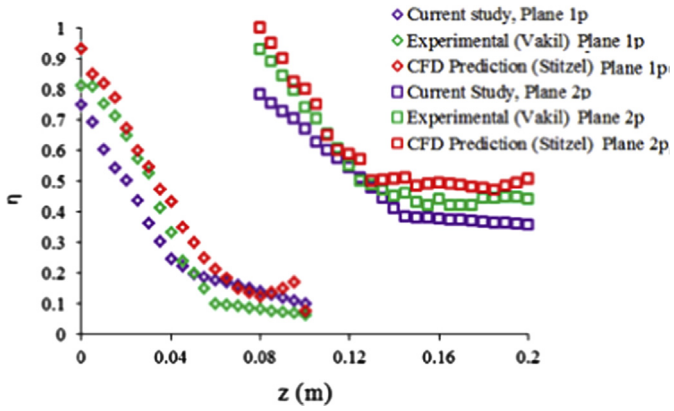

Fig. 5. The comparison of film cooling effectiveness for plane 1p and 2p along $Y/W=0.4$.

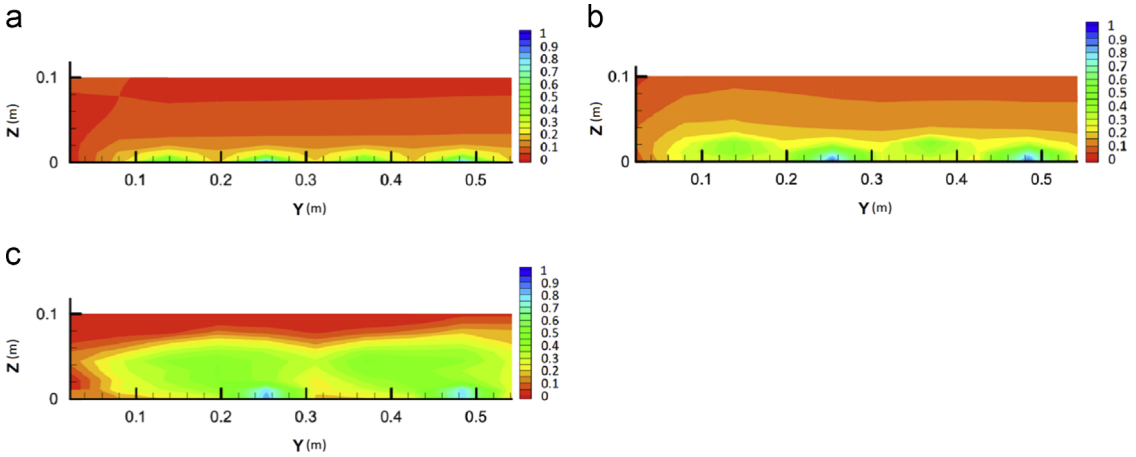

Fig. 6. Film cooling distribution for plane 0p. (a) Baseline, (b) case 2, and (c) case 3.

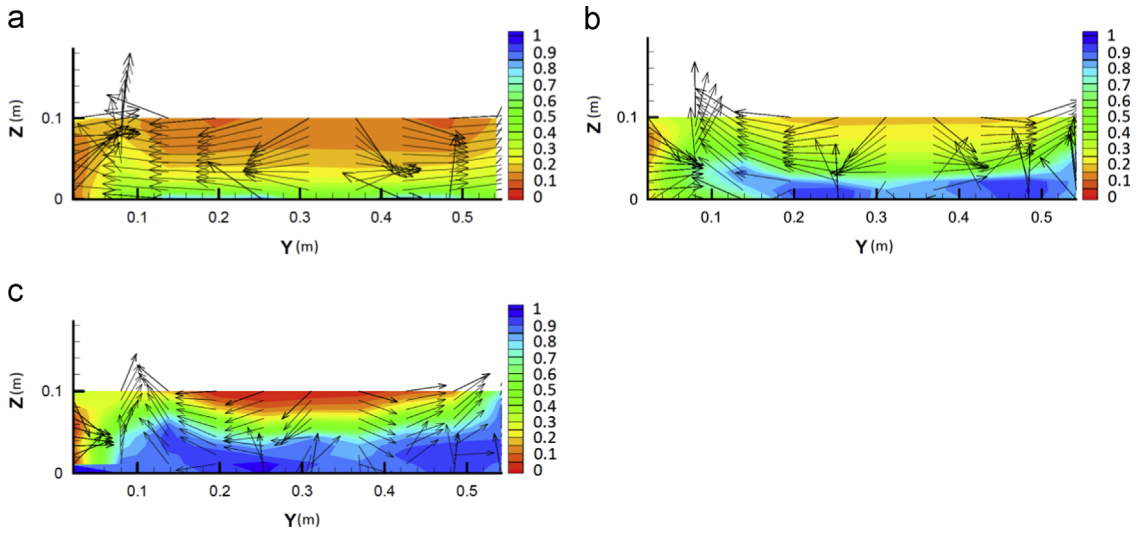

Fig. 7. The vectors of v and w with film cooling effectiveness contours for plane 1p. (a) Baseline, (b) case 2, and (c) case 3.

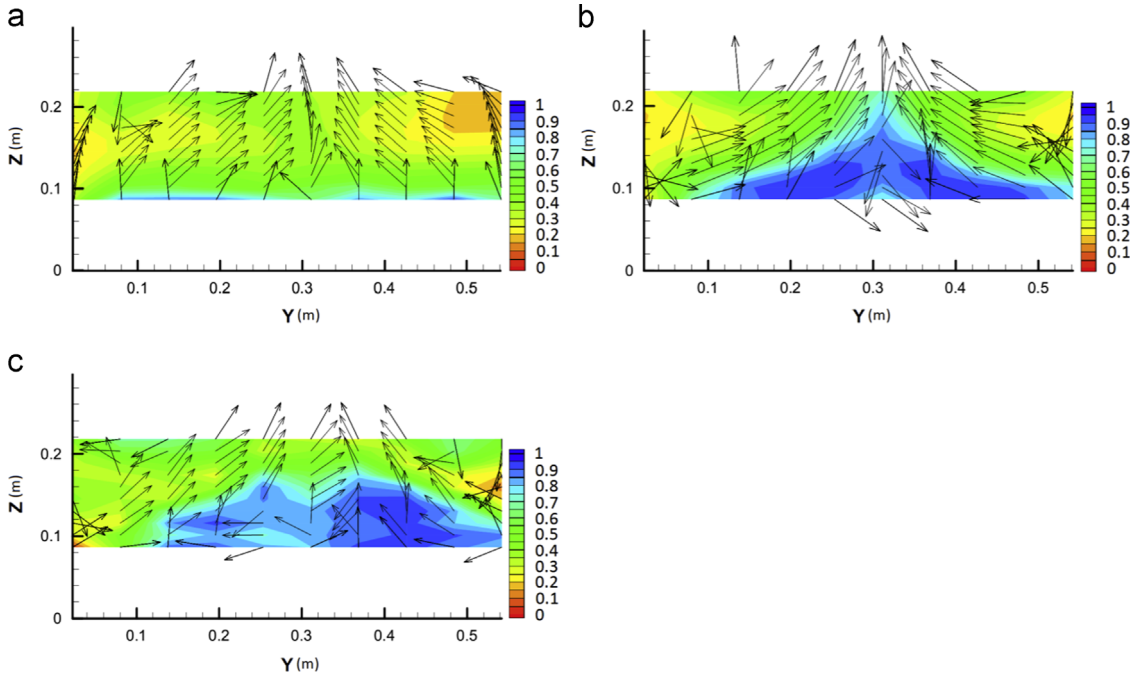

Fig. 8. Vectors of v and w overlaying film cooling effectiveness contours within plane 2p. (a) Baseline, (b) case 2, and (c) case 3.

1p are shown as well. From the middle of the temperature distribution contour, a significant movement of vortexes toward the left and right sides is found. This is the effect of dilution injection on the thermal behavior of flow. In addition, a counter rotating vortex is seen at the right side of both contours.

Fig. 8a (baseline), b (case 2) and c (case 3) show the film cooling distribution for plane 2p. It is declared from the analysis of contours that the rotating flow is seen on the left side of the figure and it is entrained along the spanwise direction. However, this rotating area is weaker for the trenched cases, especially for the trenched case with alignment angle of 90°. Overwhelmingly apparent, however, is the lack of uniformity within the combustor exiting profile at this point. Also, at the right side of Fig. 8a the hot gases covered more extended area in comparison with the trenched cases. Lastly, these figures show the v and w velocity vectors superimposed on the thermal field contours of this measurement plane. The sweeping of the coolant toward the second row of the dilution jet is visible.

Fig. 9a (baseline), b (case 2) and c (case 3) indicates the film cooling effectiveness distribution of plane 3p. The results showed that film cooling effectiveness is higher for the trenched cases. As shown in the figure, a cooler area is spread better

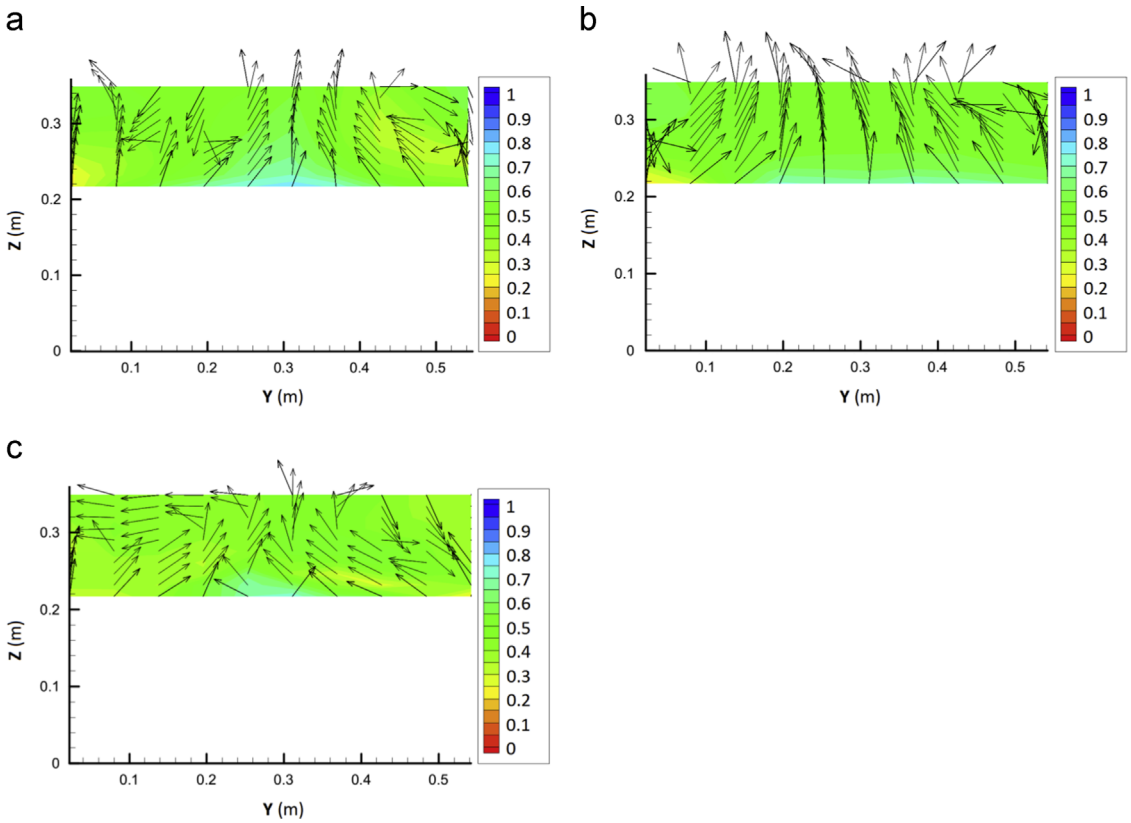

Fig. 9. The film cooling effectiveness contours with vectors of v and w for plane 3p. (a) Baseline, (b) case 2, and (c) case 3.

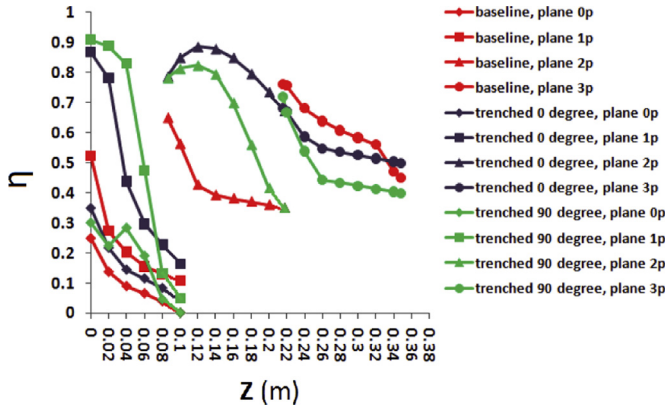

Fig. 10. The changes of film cooling effectiveness for different measurement planes and configurations.

for the trenched cases at the right side of the contour, especially for the trenched case with alignment angle of 0°. At the middle of the contour, no significant difference is seen between the contours. Also, this figure shows the velocity vectors of v and w overlying on the thermal field contours in plane 3p. A dominant vortex, rotating in the counter-clockwise direction at $0 < Y < 30$ cm as well as the vortexes rotating in the clockwise direction at 30 cm $< Y <$ 54 cm is found. However, the rotating of the vortexes is more turbulent for the trenched cases because the coolant is injected further and the interaction of the film-coolant flow is entrained by the shear forces created by the main flow.

The variation of film cooling effectiveness for different measurement planes at $Y = 30$ cm and along Z axis is shown in Fig. 10. It is declared that for plane 0p, case 3 (trenched hole with alignment angle of 90°) performs better from $Z = 0$ cm to $Z = 6$ cm, at further distance, case 2 is more effective. For plane 1p, the result is almost similar to the result of plane 0p. Also, from investigation of plane 2p, it is found that film cooling effectiveness for the trenched hole with alignment angle of 0° plays a better role and this is noticeably higher than other configurations. After that, the trenched hole with alignment angle of 90° is higher. Lastly for measurement plane of 3p, it is the baseline case that is more effective.

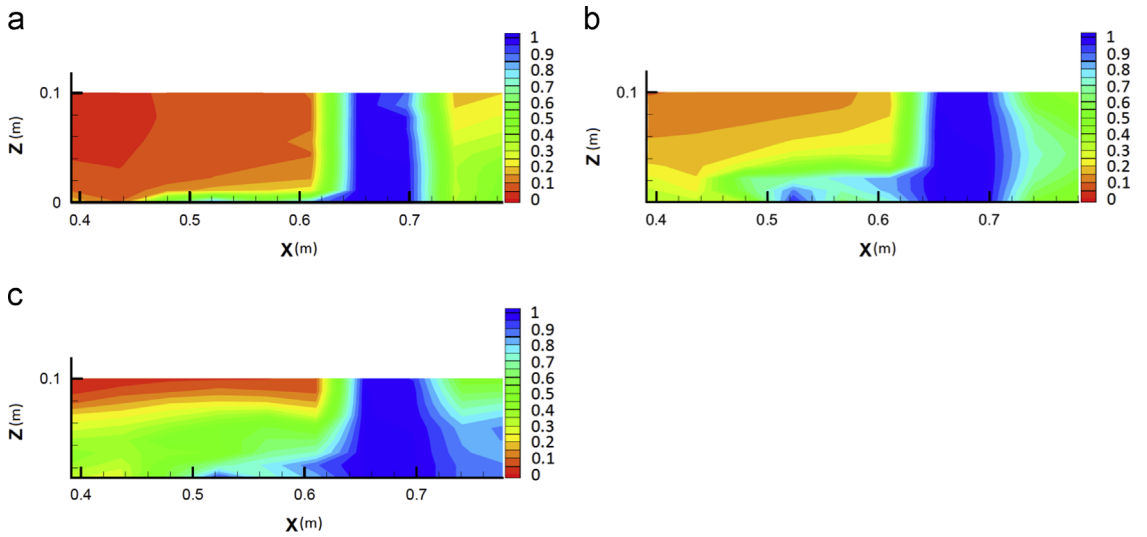

Fig. 11. The film cooling effectiveness contours for plane 0 s (a) baseline, (b) case 2, and (c) case 3.

Fig. 11a (baseline), b (case 2) and c (case 3) show the streamwise film cooling distribution through the first row of the dilution jet. Note that at the position of 60 cm $< X <$ 72 cm, the dilution jet injected into the mainstream and the coolest region is created. Furthermore, upstream the dilution jet, the hot region approximately disappears for the trenched cases and it happens due to the effects of coolant penetration from a trenched cooling hole.

4. Conclusion and recommendations

The objective of this study was to analyze the effects of different cooling hole configurations of cylindrical, row trenched holes with alignment angles of 0° and 90° at blowing ratio of 3.18 on the film cooling effectiveness at the end of the combustor simulator. In this study a three-dimensional representation of a Pratt and Whitney engine was simulated and analyzed. To sum up, the usage of trenched cooling holes significantly to development of the film cooling layer. Also, the central part of plane 2p showed intense penetration of the coolant and a thick film cooling layer creation in the trenched cases, especially for the trenched hole with alignment angle of 0°. However, the temperature adjacent to the wall and between the jets was cooler with trenching the cooling holes because by trenching the cooling holes, the coolant spread better in this area. The thermal field findings demonstrated a recirculation area developed exactly downstream of the jet where the entrainment of film cooling was caused by the dilution jet. The contours of the streamwise thermal field indicate the intense effect of trenched cooling holes and dilution injection downstream the dilution jet. Initially, the results declared that for the measurement plane of 0p, 1p and 2p trenching cooling holes have an intense effect on film cooling effectiveness especially for planes 1p and 2p as opposed to plane 3p. A comparison between experimental and computational results shows that the prediction of the film cooling for the different measurement planes exhibited a thinner film cooling layer for the current study. Based on the results and conclusions of the study, there are several recommendations to consider. In future research within this area, different configurations of trenched cooling holes and baseline case should be considered for different cooling panels. Different cooling hole arrangements affect the film cooling effectiveness at different cooling panels. The effects of different blowing ratios on the film cooling performance should be noticed as well.

References

[1] Hale CA, Plesniak MW, Ramadhyani S. Film cooling effectiveness for short film cooling holes fed by a narrow plenum. J Turbomach 2000;122:553–7.
[2] Burd SW, Simon TW. Measurements of discharge coefficients in film cooling. J Turbomach 1999;121:243–8.
[3] Stitzel S, Thole KA. Flow field computations of combustor–turbine interactions relevant to a gas turbine engine. J Turbomach 2004;126:122–9.
[4] Scrittore JJ. In: Experimental study of the effect of dilution jets on film cooling flow in a gas turbine combustor [Ph.D. thesis]. Virginia: Virginia Polytechnic Institute and State University; 160.
[5] Kianpour E, Sidik NAC, Agha Seyyed Mirza Bozorg M. Thermodynamicanalysis of flow field atthe end of combustor simulator. In: Proceedings of the AEROTECH IV conference, Kuala Lumpur, Malaysia; 2012, AMM.225.261.
[6] Kianpour E, Sidik NAC, Agha Seyyed Mirza Bozorg M. Dynamic analysis of flow field at the end of combustor simulator. J Teknol 2012;58:5–12.
[7] Aga V, Abhari RS. Influence of flow structure on compound angled film cooling effectiveness and heat transfer. J Turbomach 2011;133:031029-10–2.
[8] I-Chien L, Yun-Chung C, Pei-Pei D, Ping-Hei C. Film cooling over a concave surface through two staggered rows of compound angle holes. J Chin Inst Eng 2005;28:827–36.
[9] Yiping L, Dhungel A, Ekkad SV, Bunker RS. Effect of trench width and depth on film cooling from cylindrical holes embedded in trenches. J Turbomach 2009;131:011003-1–13.
[10] Maikell J, Bogard D, Piggush J, Kohli A. Experimental simulation of a film cooled turbine blade leading edge including thermal barrier coating effects. J Turbomach 2011;133:011014-1–7.

[11] Azzi A, Jubran BA. Influence of leading-edge lateral injection angles on the film cooling effectiveness of a gas turbine blade. J Heat Mass Transf 2004;40:501–8pp 2004;40:501–8.
[12] Rozati A, Danesh Tafti K. effect of coolant-mainstream blowing ratio on leading edge film cooling flow and heat transfer-LES investigation. J Heat Fluid Flow 2008;29:857–73.
[13] Lawson SA, Thole KA. Simulations of multiphase particle deposition on end wall film-cooling holes in transverse trenches. J Turbomach 2012;134:051040-1–10.
[14] Tarchi L, Facchini B, Maiuolo F, Coutandin D. Experimental investigation on the effects of a large recirculating area on the performance of an effusion cooled combustor liner. J Eng Gas Turbines Power 2012;134:041505-1–9.
[15] Sundaram N, Thole KA. Bump and trench modifications to film-cooling holes at the vane-end wall junction. J Turbomach 2008;130:041013-1–9.
[16] Milanes DW, Kirk DR, Fidkowski KJ, Waitz IA. Gas turbine engine durability impacts of high fuel-air ratio combustors: near wall reaction effects on film-cooled backward-facing step heat transfer. J Eng Gas Turbines Power 2006;128:318–25.
[17] Liang LC, Hui RZ, Jiang BT, Du XC. Film cooling performance of converging slot-hole rows on a gas turbine blade. Int J Heat Mass Transf 2010;53:5232–41.
[18] Liang LC, Hui RZ, Jiang BT, Du XC. Film cooling performance of converging-slot holes with different exit–entry area ratios. J Turbomach 2011;133:011020-1–011020-11.
[19] Somawardhana RP, Bogard DG. Effects of obstructions and surface roughness on film cooling effectiveness with and without a transverse trench. J Turbomach 2009;131:011010-1–8.
[20] Vakil SS, Thole KA. Flow and thermal field measurements in a combustor simulator relevant to a gas turbine aero engine. J Eng Gas Turbines Power 2005;127:257–67.
[21] Shuping C. Film cooling enhancement with surface restructure [Ph.D. thesis]. Pennsylvania.University of Pittsburgh; 150.
[22] Harrison KL, Dorrington JR, Dees JE, Bogard DG, Bunker RS. Turbine airfoil net heat flux reduction with cylindrical holes embedded in a transverse trench. J Turbomach 2009;131:011012-1–8.
[23] Barringer MD, Richard OT, Walter JP, Stitzel SM, Thole KA. Flow field simulations of a gas turbine combustor. J Turbomach 2002;124:508–16.